

In vitro metabolic engineering of hydrogen production at theoretical yield from sucrose



Suwan Myung^{a,b}, Joseph Rollin^a, Chun You^a, Fangfang Sun^{a,c}, Sanjeev Chandrayan^d, Michael W.W. Adams^{d,e}, Y.-H. Percival Zhang^{a,b,c,*}

^a Biological Systems Engineering Department, Virginia Tech, 304 Seitz Hall, Blacksburg, VA 24061, USA

^b Institute for Critical Technology and Applied Science (ICTAS), Virginia Tech, Blacksburg, VA 24061, USA

^c Cell Free Bioinnovations Inc. (CFB9), Blacksburg, VA 24060, USA

^d Department of Biochemistry and Molecular Biology, University of Georgia, Athens, GA 30602, USA

^e DOE BioEnergy Science Center (BESC), Oak Ridge, TN 37831, USA

ARTICLE INFO

Article history:

Received 26 January 2014

Received in revised form

3 May 2014

Accepted 5 May 2014

Available online 13 May 2014

Keywords:

Innovative biomanufacturing
In vitro metabolic engineering
Hydrogen
In vitro synthetic biology
Sucrose

ABSTRACT

Hydrogen is one of the most important industrial chemicals and will be arguably the best fuel in the future. Hydrogen production from less costly renewable sugars can provide affordable hydrogen, decrease reliance on fossil fuels, and achieve nearly zero net greenhouse gas emissions, but current chemical and biological means suffer from low hydrogen yields and/or severe reaction conditions. An in vitro synthetic enzymatic pathway comprised of 15 enzymes was designed to split water powered by sucrose to hydrogen. Hydrogen and carbon dioxide were spontaneously generated from sucrose or glucose and water mediated by enzyme cocktails containing up to 15 enzymes under mild reaction conditions (i.e. 37 °C and atm). In a batch reaction, the hydrogen yield was 23.2 mol of dihydrogen per mole of sucrose, i.e., 96.7% of the theoretical yield (i.e., 12 dihydrogen per hexose). In a fed-batch reaction, increasing substrate concentration led to 3.3-fold enhancement in reaction rate to 9.74 mmol of H₂/L/h. These proof-of-concept results suggest that catabolic water splitting powered by sugars catalyzed by enzyme cocktails could be an appealing green hydrogen production approach.

© 2014 International Metabolic Engineering Society. Published by Elsevier Inc. All rights reserved.

1. Introduction

Concerns about the depletion of fossil fuels and accumulation of greenhouse gases motivate the use of renewable energy sources and enhanced energy utilization efficiencies. Hydrogen is widely believed to be one of the best future energy carriers and energy storage compounds, especially in the hypothetical hydrogen economy, mainly because of higher energy conversion efficiencies through fuel cells and fewer pollutants generated in end users. Full development of the hydrogen economy requires breakthroughs in hydrogen production, storage, transportation and distribution (Armaroli and Balzani, 2011; Zhang, 2009). Also, hydrogen, which is mainly produced from natural gas, is one of the most important chemical commodities used for making fertilizers and refining liquid transportation fuels (Armaroli and Balzani, 2011; Navarro et al., 2007). The future of energy chains depends on innovative breakthroughs in the design of cheap, sustainable, and efficient systems for the harvesting, conversion, and storage of renewable energy sources, such as solar energy and carbohydrates (Artero et al., 2011).

Sunlight-driven water splitting for the production of hydrogen through artificial photosynthesis can be implemented by using natural photosynthetic systems, namely hydrogenases and photosystem II (Barber and Tran, 2013; Ducat et al., 2011; Wang et al., 2012; Wells et al., 2011); artificial photosynthetic systems based on photosensitizers/semiconductors/photocatalysts (Artero et al., 2011; Mubeen et al., 2013); and their hybrids (Iwuchukwu et al., 2009). Because solar energy is intermittent, broad wavelength electromagnetic radiation with an average energy concentration of ~170 W/m², great challenges result from solar energy harvesting, high-efficiency conversion under different strength insulations, and gaseous product collection from large-surface solar energy harvesting systems (Barber and Tran, 2013). Therefore, technologies for water splitting powered by direct solar energy are still far from practical applications (Armaroli and Balzani, 2011; Artero et al., 2011; Esswein and Nocera, 2007).

In vitro metabolic engineering or cell-free metabolic engineering has been used to understand complicated cellular metabolisms (Hodgman and Jewett, 2012; Jung and Stephanopoulos, 2004; Zhang, 2010). Recently, it is under investigation for its manufacturing potentials (Hodgman and Jewett, 2012; Rollin et al., 2013; Swartz, 2013), such as the synthesis of special proteins (Goerke et al., 2008; Hodgman and Jewett, 2012) and high-value polysaccharides (Xu et al., 2011), as well as the production of biofuels and bioelectricity (Guterl et al., 2012; Krutsakorn et al., 2013; Martín del Campo et al., 2013; Zhu

* Corresponding author at: Biological Systems Engineering Department, Virginia Tech, 304 Seitz Hall, Blacksburg, VA 24061, USA. Fax: +1 540 231 3199.

E-mail addresses: ypzhang@vt.edu, yhpzhang@gmail.com (Y.-H.P. Zhang).

et al., 2014), biochemicals (Bujara et al., 2011; Korman et al., 2014; Wang et al., 2011), and even potential food/feed (You et al., 2013). In vitro metabolic engineering feature several compelling biomanufacturing advantages, such as high product yields without the formation of by-products or the synthesis of cell mass; fast reaction rates without cell membrane (Hodgman and Jewett, 2012; Zhu et al., 2014); the tolerance of toxic products or substrates (Guterl et al., 2012; Wang et al., 2011); broad reaction conditions such as high temperature, low pH, the presence of organic solvents or ionic liquids (Panke et al., 2004); easy product separation; the implementation of non-natural reactions, for example, enzymatic transformation of cellulose to starch (You et al., 2013); among others.

Sucrose is the primary product of plant photosynthesis and then converted to other plant components. Sucrose is a disaccharide composed of glucose linked to fructose via an ether bond between C1 on the glucosyl subunit and C2 on the fructosyl unit. It is the most abundant disaccharide and approximately 168 million metric tons was produced from sugarcane, sugar beet, sorghum, and so on, in 2011 (Qi et al., 2014). Although its price varied greatly by several folds in the past 10 years (Qi et al., 2014), sucrose is among the cheapest fermentable sugars. When feedstock cost is considered only, hydrogen production from sucrose might be more cost competitive than from starch. For example, Brazil produces the lowest-cost ethanol compared to ethanol produced from starch and lignocellulosic biomass sugars.

Water splitting powered by sugars instead of insolation is promising due to potentially high reaction rates and easy product collection and separation. However, natural and metabolically engineered hydrogen-producing microorganisms cannot produce high-yield hydrogen from sugars due to the Thauer limit (i.e., 4 mol of hydrogen per mole of hexose) (Agapakis et al., 2010; Chou et al., 2008; Ducat et al., 2011; Maeda et al., 2012). To break the constraints of microorganisms, in vitro metabolic engineering can be used to implement complicated biological reactions by the in vitro assembly of numerous (purified) enzymes or cell extracts, a system that insulates biocatalyst preparation from product formation in space and time. Woodward and his co-workers demonstrated the production of 11.6 mol of hydrogen from 1 mol of glucose 6-phosphate (Woodward et al., 2000) (i.e., 12H₂ can be produced from one glucose 6-phosphate and seven H₂O), but the high cost of the substrate prevented its potential application. Later, we proposed the utilization of the 1,4-glycosidic bond energy stored between two anhydroglucose units of polysaccharides (e.g., starch and cellodextrins) mediated by glucan phosphorylases plus recycled phosphate ions for producing glucose 6-phosphate without costly ATP (Ye et al., 2009; Zhang et al., 2007). As a result, nearly 12 mol of hydrogen was produced from each glucose unit of polysaccharides, where the theoretical yield of hydrogen was 12H₂ per hexose (Ye et al., 2009; Zhang et al., 2007). However, 1 mol of glucose unit per mole of polysaccharides cannot be utilized. When the degree of polymerization of polysaccharides and oligosaccharides is small, a significant fraction of hexose cannot be utilized for hydrogen production.

In this study, a novel in vitro non-natural enzymatic pathway comprised of 15 enzymes was designed to convert sucrose, glucose or fructose to high-yield hydrogen without the use of costly ATP. Also, a fed-batch reaction was run for enhancing hydrogen generation rates at high substrate concentrations.

2. Materials and methods

2.1. Chemicals and strains

All chemicals were reagent grade, purchased from Sigma-Aldrich (St. Louis, MO) and Fisher Scientific (Pittsburgh, PA), unless otherwise noted. Avicel PH105, microcrystalline cellulose, was purchased from FMC (Philadelphia, PA). The genomic DNA sample

of *Thermus thermophilus* HB27 was purchased from the American Type Culture Collection (Manassas, VA). *E. coli* BL21 Star (DE3) (Invitrogen, Carlsbad, CA) containing a protein expression plasmid was used to produce the recombinant protein. Luria–Bertani (LB) medium was used for *E. coli* cell growth and recombinant protein expression supplemented with 100 µg/mL ampicillin or 50 µg/mL kanamycin. Oligonucleotides were synthesized by Integrated DNA Technologies (Coraville, IA) and Fisher Scientific. Xylose isomerase (G4166) from *Streptomyces murinus* and sucrose phosphorylase (S0937) from *Leuconostoc mesenteroides* were purchased from Sigma. Recombinant hydrogenase SH1 was produced and purified from *Pyrococcus furiosus* (Chandrayan et al., 2012).

2.2. Plasmid construction

Two new plasmids were prepared for producing *T. thermophilus* HB27 fructose-bisphosphate aldolase (TtcALD) and transketolase (TtcTK) in *E. coli* BL21 (DE3). Plasmids pET20b-ttc-ald and pET20b-ttc-tk were constructed by the newly developed restriction enzyme-free, ligase-free and sequence-independent simple cloning method (You et al., 2012b). The other plasmids were described elsewhere (Martín del Campo et al., 2013; Wang et al., 2011).

The 918-bp DNA fragment containing the open reading frame (ORF) of the fructose-bisphosphate aldolase (Ttc1414) was amplified by PCR from the genomic DNA of *T. thermophilus* HB27 using a pair of primers (forward primer: 5'-TAACT TTAAG AAGGA GATAT ACATA TGCTG GTAAC GGGTC TAGAG ATCT-3'; reverse primer: 5'-AGTGG TGGTG GTGGT GGTGC TCGAG AGCCC GCCCC ACGGA GCCGA AAAGC-3'). The vector backbone of pET20b was amplified by PCR using a pair of primers (forward primer: 5'-GCTTT TCGGC TCCGT GGGGC GGGCT CTCGA GCACC ACCAC CACCA CCACT-3'; reverse primer: 5'-AGATC TCTAG ACCCG TTACC AGCAT ATGTA TATCT CCTTC TTTAA GTTAA-3'). The PCR products were purified using the Zymo Research DNA Clean & Concentrator Kit (Irvine, CA). The insertion DNA fragment and vector backbone were assembled by prolonged overlap extension PCR (You et al., 2012b), and then the PCR product (DNA multimer) was directly transformed into *E. coli* TOP10 cells, yielding the desired plasmid.

The 1956-bp DNA fragment containing the ORF of the transketolase (Ttc1896) was amplified by PCR from the genomic DNA of *T. thermophilus* HB27 using a pair of primers (forward primer: 5'-TTAAC TTAA GAAGG AGATA TACAT ATGAA GGAGA CGCGG GACCT AGAGA-3'; reverse primer: 5'-GATCT CAGTG GTGGT GGTGG TGGTG CACCA GGGAG AGGAA GGCCT CCGCC-3'). The vector backbone of pET20b was amplified by PCR using a pair of primers (forward primer: 5'-GGCGG AGGCC TTCT CTCCC TGGTG CACCA CCACC ACCAC CACTG AGATC-3'; reverse primer: 5'-TCTCT AGGTC CCGCG TCTCC TTCAT ATGTA TATCT CCTTC TTTAA GTTAA-3'). The insertion DNA fragment and vector backbone DNA fragment was assembled to the desired plasmid by using prolonged overlap extension PCR (You et al., 2012b).

2.3. Recombinant protein expression and purification

For the preparation of recombinant proteins: two hundred milliliters of LB culture containing 50 µg/mL of kanamycin or 100 µg/mL of ampicillin in 1-L Erlenmeyer flasks was incubated with a rotary shaking rate of 250 rpm at 37 °C. When the absorbance (A₆₀₀) reached ca. 0.6–1.2, recombinant protein expression was induced by adding isopropyl-β-D-thiogalactopyranoside (IPTG) (0.01–0.1 mM, final concentration). The culture was incubated at 37 °C for 4 h or at 18 °C for 20 h. The cells were harvested by centrifugation at 4 °C, washed twice by 50 mM of Tris–HCl buffer (pH 7.5), and re-suspended in a 15 mL of 30 mM Tris–HCl buffer (pH 7.5) containing 0.5 M of NaCl and 1 mM of EDTA. The cell pellets were lysed using a Fisher Scientific Sonic

Dismembrator Model 500 (5-s pulse on and off, total 360 s, at 20% amplitude) in an ice bath. After centrifugation, the target proteins were purified through several methods, such as His-tag purification, CBM-intein self cleavage or ethylene glycol elution of CBM-tagged enzyme, and heat treatment. The His-tagged proteins G6PDH, 6PGDH, TK, and TAL were purified by Ni-charged resins (Bio-Rad, Profinity IMAC Ni-Charged Resin). PGM, FBP, PGI, CBM-PPGK were purified by intein self cleavage method or ethylene glycol elution from the fusion proteins CBM-intein-PGM (Wang and Zhang, 2010), CBM-intein-FBP (Myung et al., 2010), CBM-intein-PGI (Myung et al., 2011), and CBM-PPGK (Liao et al., 2012), respectively. RPI, RPE, TIM and ALD were purified by heat precipitation at 80 °C for 20 min (Myung and Zhang, 2013; Sun et al., 2012) (Table 1).

2.4. Enzyme activity assays

Thermobifida fusca CBM-PPGK activity was measured based on the generation of glucose 6-phosphate from polyphosphate and glucose in a 50-mM HEPES buffer (pH 7.5) containing 4 mM MgCl₂, 5 mM D-glucose, and 1 mM polyphosphate at 50 °C for 5 min (Liao et al., 2012). The specific activity of CBM-PPGK was 55 U/mg at 37 °C.

Clostridium thermocellum PGM activity was measured in a 50 mM HEPES buffer (pH 7.5) containing 5 mM glucose 1-phosphate, 5 mM MgCl₂ and 0.5 mM MnCl₂ at 37 °C for 5 min (Wang and Zhang, 2010). The specific activity of PGM was 260 U/mg at 37m°C.

Geobacillus stearothermophilus G6PDH activity was measured in 100 mM HEPES buffer (pH 7.5) containing 5 mM MgCl₂ and 0.5 mM MnCl₂, 2 mM glucose 6-phosphate and 0.67 mM NADP⁺. The increase in absorbance at 340 nm was measured in 5 min. The specific activity was 1.1 U/mg at 37m°C (Zhu et al., 2014).

Morella thermoacetica 6PGDH activity was measured in a 50 mM HEPES buffer (pH 7.5) containing 2 mM 6-phosphogluconate, 1 mM NADP⁺, 5 mM MgCl₂, 0.5 mM MnCl₂, at 37 °C for 5 min (Zhu et al.,

2014). The reaction product NADPH was measured at 340 nm. The specific activity was 15 U/mg.

T. maritima RPI activity was assayed by a modified Dische's cysteine-carbazole method. The specific activity was 190 U/mg at 37m°C (Sun et al., 2012).

T. maritima RPE activity was determined on a substrate D-ribulose 5-phosphate as described previously (Wang et al., 2011). The specific activity of RPE was 1.42 U/mg at 50m°C.

T. thermophilus TK activity assay was measured on the substrates of D-xylulose 5-phosphate and D-ribose 5-phosphate. The reactions were carried out in a 50 mM Tris/HCl pH 7.5 buffer containing 0.8 mM D-xylulose 5-phosphate, 0.8 mM D-ribose 5-phosphate, 15 mM MgCl₂, 0.03 mM Thiamine pyrophosphate, 0.14 mM NADH, 60 U/mL of TIM and, 20 U/mL of glycerol 3-phosphate dehydrogenase (Wang et al., 2011). The specific activity of TK was 1.3 U/mg at 25 °C.

T. maritima TAL activity assay was carried as reported previously and it has a specific activity of 13 U/mg at 37m°C (Huang et al., 2012).

T. thermophilus TIM activity was measured in 100 mM HEPES pH 7.5 containing 10 mM MgCl₂, 0.5 mM MnCl₂ at 60 °C for 5 min containing 2 mM D-glyceraldehyde 3-phosphate (You et al., 2012a). The reaction was stopped with HClO₄ and neutralized with KOH. The product dihydroxyacetone phosphate was measured by using glycerol 3-phosphate dehydrogenase in the presence of 0.15 mM NADH at 25 °C (You et al., 2012a). The specific activity at these conditions was 870 U/mg at 60 °C.

T. thermophilus ALD was assayed in a 100 mM HEPES pH 7.5 containing 10 mM MgCl₂, 0.5 mM MnCl₂ at 60 °C for 5 min with 2 mM of D-glyceraldehyde 3-phosphate in the presence of TIM, FBP, and PGI. The reaction was stopped with HClO₄ and neutralized with KOH (You and Zhang, 2014). The product glucose 6-phosphate was analyzed at 37 °C with liquid glucose reagent set (Pointe scientific). The specific activity of ALD was 36 U/mg at 60 °C.

T. maritima FBP activity was determined based on the release of phosphate and its specific activity of FBP at 37B°C was 6 U/mg (Myung et al., 2010).

Table 1
The list of enzymes and their properties for the loading to generation of hydrogen from sucrose.

No.	Enzyme	Enzyme catalog	Source/(ORF) ^a	Plasmid name	Purification ^b	Sp. Act. ^c (U/mg)	Load (U/ mL)	Ref.
1	Sucrose phosphorylase (SP)	EC 2.4.1.7	<i>L. mesenteroides</i>	N/A	Sigma	102	5	–
2	Xylose isomerase (XI)	EC 5.3.1.5	<i>S. murinus</i>	N/A	Sigma	0.80	5	–
3	Polyphosphate glucokinase (PPGK)	EC 2.7.1.63	REE, Tfu1811	pCBM-ppgk	CBM-tag	55	5	Liao et al. (2012)
4	Phosphoglucomutase (PGM)	EC 5.4.2.2	REE, Cthe1265	pCl-cthe-pgm	CBM-intein self cleavage	260	5	Wang and Zhang (2010)
5.	Glucose 6-phosphate dehydrogenase (G6PDH)	EC 1.1.1.49	REE, GsG6PDH	pGsG6PDH	His-tag	29	5	Zhu et al. (2012)
6.	6-Phosphogluconate dehydrogenase (6PGDH)	EC 1.1.1.44	REE, Moth1283	pET33b-moth-6pgdh	His-tag	15	5	Wang et al. (2011)
7.	Ribose 5-phosphate isomerase (RPI)	EC 5.3.1.6	REE, Tm1080	pET20b-r5pi	Heat precipitation	190	1	Sun et al. (2012)
8	Ribulose 5-phosphate 3-epimerase (RPE)	EC 5.1.3.1	REE, Tm1718	pET20b-tm-rpe	Heat precipitation	0.60	1	Martin del Campo et al. (2013)
9	Transketolase (TK)	EC 2.2.1.1	REE, Ttc1896	pET20b-ttc-tk	His-tag	3.0	1	This study
10	Transaldolase (TAL)	EC 2.2.1.2	REE, Tm0295	pET28a(+)-tal	His-tag	13	1	Huang et al. (2012)
11	Triose phosphate isomerase (TIM)	EC 5.3.1.2	REE, Ttc0581	pET33b-ttc-tim	Heat precipitation	180	1	Wang et al. (2011)
12	Fructose-bisphosphate aldolase (ALD)	EC 4.1.2.13	REE, Ttc1414	pET20b-ttc-ald	Heat precipitation	7.3	1	This study
13	Fructose bisphosphatase (FBP)	EC 3.1.3.11	REE, Tm1415	pCl-tm-fbp	CBM-intein self cleavage	6.0	1	Myung et al. (2010)
14	Phosphoglucose isomerase (PGI)	EC 5.3.1.9	REE, Cthe0217	pCl-ttc-pgi	CBM-intein self cleavage	500	1	Myung et al. (2011)
15	Hydrogen dehydrogenase (H ₂ ase)	EC 1.1.2.1.3	<i>P. furiosus</i>	N/A	Strep-tagII	0.5	1	Chandrayan et al. (2012)

^a REE, recombinant expression in *E. coli*; ORF, open reading fragment.

^b His-tag, purified by His-tag of recombinant protein binding with nickel resin; Sigma, purchased from Sigma; CBM-tage, purification by CBM binding with RAC followed by ethylene glycol elution method; CBM-intein, purified by CBM binding with RAC followed by self cleavage of intein; *Strep-tagII*, purification by the recombinant enzyme containing the *Strep-tagII* using a *StrepTactin* column.

^c Specific activity at 37 °C; relatively standard deviations of specific activities were less than 10%.

C. thermocellum PGI activity was assayed at 37°C in 100 mM HEPES (pH 7.5) containing 10 mM MgCl₂ and 0.5 mM MnCl₂ with 5 mM fructose 6-phosphate as substrate (Myung et al., 2011). After 3 h the reaction was stopped with HClO₄ and neutralized with KOH. The product glucose 6-phosphate was analyzed at 37 °C with liquid glucose hexokinase kit (Pointe scientific). The specific activity of PGI at 37w°C was 500 U/mg.

2.5. Preparation of the enzyme cocktail

The reaction buffer was 100 mM HEPES (pH 7.5) containing 4 mM NADP⁺, 0.5 mM thiamine pyrophosphate, 10 mM MgCl₂ and 0.5 mM MnCl₂ unless otherwise noted. The concentrations of sucrose, phosphate, and polyphosphate ((P_i)₆, sodium hexametaphosphate) were 2 mM, 4 mM and 4 mM, respectively. The enzyme loadings were added as shown in Table 1.

10 mg of immobilized XI per mL of the reaction volume were placed in the reaction vessel, followed by addition of all enzymes, cofactor, P_i, and (P_i)₆. For the protection against microbial growth, 50 µg/mL of kanamycin was added as an antibiotic. To start the reaction, sucrose was added. The reactor was sealed and magnetic agitation was started, along with the flow of nitrogen carrier gas at a flow rate of 30 mL/min and hydrogen thermal conductivity detector data acquisition. When the oxygen inside the reactor was completely evacuated for ensuring hydrogenase to be active and when a significant fraction of initially-added NADP⁺ was converted to NADPH that was converted to hydrogen by hydrogenase, hydrogen production started. During the whole experiment, temperature, carrier gas flow, and hydrogen signals were monitored. To increase the dihydrogen rate, three different concentrations of sucrose were introduced sequentially in the same reactor. Sucrose concentration (i.e., 4, 10, and 50 mM) was increased stepwise when the maximum dihydrogen rate was reached. P_i (i.e., 4, 10, and 40 mM) and (P_i)₆ (i.e., 4, 10, and 20 mM) were also added according to the sucrose concentration.

2.6. System for hydrogen detection

The experiments were carried out in a continuous flow system, which was purged with ultrapure nitrogen (Airgas) (Martín del Campo et al., 2013; Ye et al., 2009; Zhang et al., 2007). Hydrogen evolution was detected with a tin oxide thermal conductivity sensor (Figaro TGS 822, Osaka, Japan) that was previously calibrated with in-line flow-controllers and ultrapure hydrogen (Airgas). The working volume of the reactor was kept constant by humidifying the carrier gas and controlling the rate of condensation. The temperature of the reactor was controlled at 37 °C (Thermo Scientific, NESLAB RTE) and the temperature of the condenser was 20 °C, which were controlled by recirculation thermal baths (Fisher Scientific, Isotemp Refrigerated Circulator Bath Model 3016D). Data collection was conducted by Ni-module NI USB-6210 (National Instruments Corp., Austin TX) and analyzed by LabView SignalExpress 2009. The integrated molar/molar yield of hydrogen (Y_{H₂}) is calculated as

$$Y_{H_2} = \frac{\int r_{H_2} dt}{24 \times \Delta \text{Sucrose}}$$

in which r_{H_2} is the volumetric production rates in terms of mmol of H₂ per liter of reaction volume per hour and Δ Sucrose is the consumed mmole concentration of sucrose per liter. Remaining sucrose concentration was measured by the Sigma glucose and sucrose enzymatic kit.

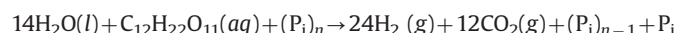
2.7. Other assays

Mass protein concentration was measured by the Bio-Rad modified Bradford protein kit with bovine serum albumin as a standard protein. 12–15% SDS-PAGE was performed in the Tris-glycine buffer to check the purity of recombinants as described elsewhere.

3. Results

3.1. Pathway design

We designed a synthetic enzymatic pathway for water splitting powered by sucrose, glucose, or fructose (Fig. 1a). Sucrose is usually hydrolyzed to glucose and fructose mediated by sucrase so that the bond energy between the linkage of fructose and glucose is dissipated. To minimize the use of phosphoryl group donors, sucrose in the presence of phosphate can be phosphorylated to fructose and glucose-1-phosphate mediated by sucrose phosphorylase (EC 2.4.1.7). Fructose can be isomerized to glucose mediated by glucose (xylose) isomerase (EC 5.3.1.5). To phosphorylate glucose without ATP, a polyphosphate-strict glucokinase (EC 2.7.1.63) is used to convert glucose to glucose 6-phosphate by transferring a terminal phosphate group from polyphosphate (Liao et al., 2012). At the same time, glucose 1-phosphate generated by sucrose phosphorylase is converted to glucose 6-phosphate mediated by phosphoglucomutase (EC 5.4.2.2). As a result, one molecule of sucrose can generate 2 mol of glucose 6-phosphate at a cost of one phosphoryl group donated from polyphosphate. Via two cascade redox enzymes in the oxidative pentose phosphate pathway: one water and one glucose 6-phosphate mediated by glucose 6-phosphate dehydrogenase and 6-phosphogluconate dehydrogenase, can generate two NADPH, one ribulose 5-phosphate and one CO₂ (Nelson and Cox, 2008). In it, one water is added in the step from 6-phosphogluconolactone to 6-phosphogluconate (Nelson and Cox, 2008). Then ribulose 5-phosphate plus 1/6 water can be regenerated back to 5/6 glucose 6-phosphate through the non-oxidative pentose phosphate pathway and gluconeogenesis pathway containing 10 enzymes (Fig. 1b). When the 15 enzymes are put in an aqueous medium containing sucrose and polyphosphate in one vessel, 14 mol of water can be catabolically split into 24 mol of dihydrogen and 12 mol of CO₂, powered by 1 mol of sucrose as shown the following equation



Polyphosphate is a very low-cost phosphate donor with a degree of polymerization ranging from several or up to thousands because it can be produced from low-concentration phosphate-containing waste water by using polyphosphate-accumulating microorganisms (Kuroda et al., 2001). In Japan polyphosphate recycled from waste water treatment facilities is used as fertilizers. In China, ammonium polyphosphate is sold as a fertilizer.

This designed reaction was spontaneous and endothermic, similar to the cases of hydrogen production from starch (Zhang et al., 2007), cellulosic materials (Ye et al., 2009), and xylose (Martín del Campo et al., 2013). It means that low-temperature thermal energy, which may be obtained from air conditioners, refrigerators, and fuel cells, can be converted to hydrogen energy via the enzyme cocktails. In contrast, none of chemical catalysis can convert low-temperature thermal energy to useful chemical energy.

3.2. Recombinant enzyme preparation

In the past several years, we tried to clone, express, and purify all thermoenzymes to prolong the life time of enzyme cocktails. Twelve recombinant thermophilic enzymes were expressed in *E.*

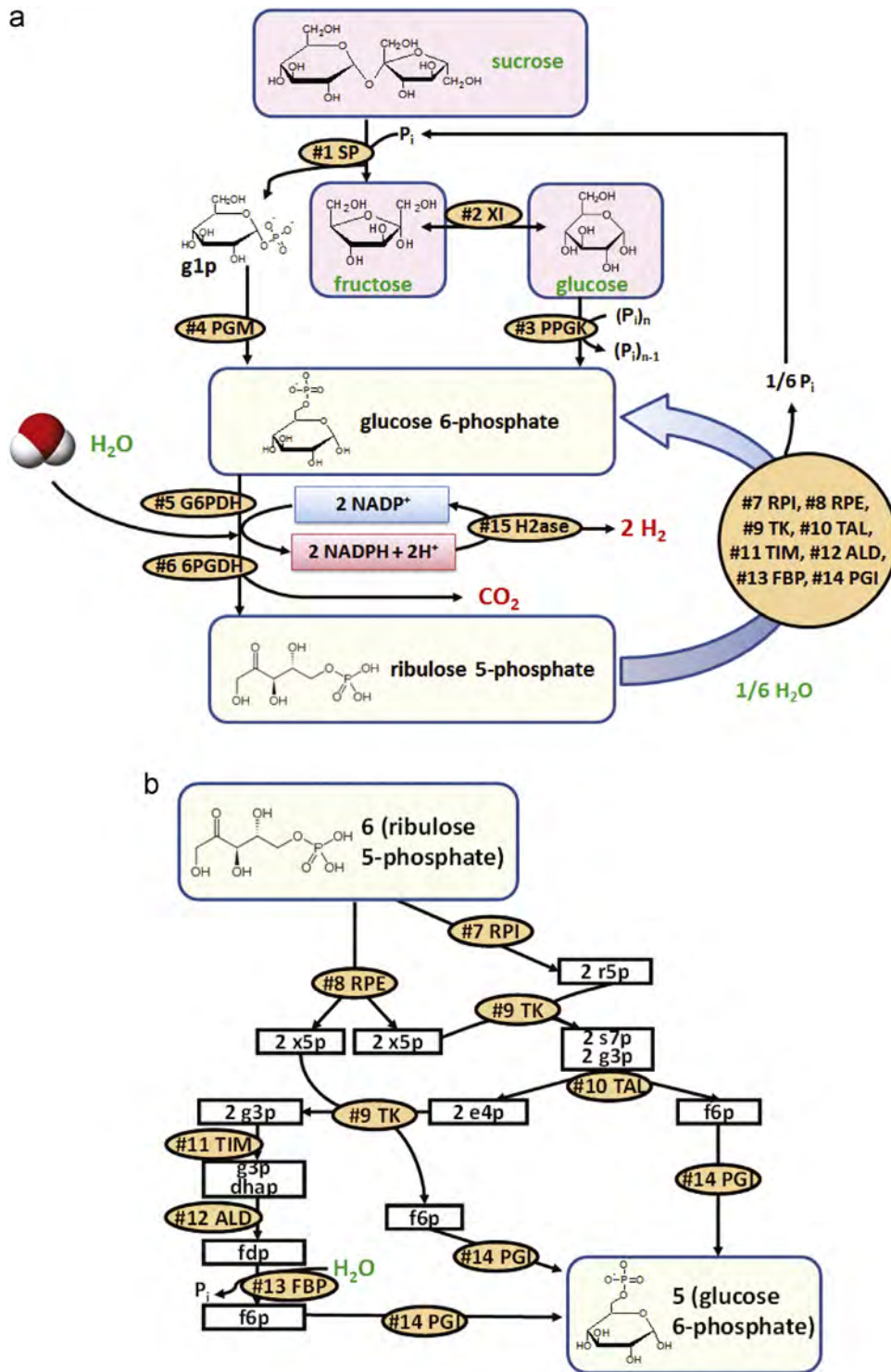


Fig. 1. (a) The scheme of the entire synthetic enzymatic pathway for dihydrogen production from sucrose, glucose or fructose, and water. The enzymes are no. 1 SP, sucrose phosphorylase; no. 2 XI, xylose isomerase; no. 3 PPGK, polyphosphate glucokinase (PPGK); no. 4 PGM, phosphoglucomutase; no. 5, G6PDH, glucose-6-phosphate dehydrogenase; no. 6 6PGDH, 6-phosphogluconate dehydrogenase; no. 7, RPI, ribose 5-phosphate isomerase; no. 8, RPE, ribulose-5-phosphate 3-epimerase; no. 9 TK, transketolase; no. 10 TAL, transaldolase; no. 11 TIM, triose phosphate isomerase; no. 12 ALD, (fructose-bisphosphate) aldolase; no. 13 FBP, fructose bisphosphatase; no. 14 PGI, phosphoglucomutase; and no. 15 H₂ase, hydrogenase. P_i and (P_i)_n are inorganic phosphate and polyphosphate with a degree of polymerization of *n*. (b) The partial synthetic pathway that regenerate five molecules of glucose 6-phosphate from six molecules of ribulose 5-phosphate. The metabolites are: g1p, glucose-1-phosphate; g6p, glucose-6-phosphate; ru5p, ribulose-5-phosphate; x5p, xylulose-5-phosphate; r5p, ribose-5-phosphate; s7p, sedoheptulose-7-phosphate; g3p, glyceraldehyde-3-phosphate; e4p, erythrose-4-phosphate; dhap, dihydroxyacetone phosphate; fdp, fructose-1,6-diphosphate; f6p, fructose-6-phosphate.

coli BL21(DE3) and purified through several methods (Table 1). Sucrose phosphorylase and xylose isomerase were purchased from Sigma-Aldrich and a recombinant non-membrane hydrogenase was isolated from a hyperthermophilic archaeon *P. furiosus*

(Chandrayan et al., 2012). Four enzymes (i.e., nos. 7, 8, 11, and 12) were purified by using heat precipitation at 80 °C for 20 min; another four enzymes (i.e., nos. 5, 6, 9, and 10) were purified by using their His-tag on nickel-charged resin; the other four

enzymes (i.e., nos. 3, 4, 13, and 14) containing a cellulose-binding module (CBM) tag, were purified through adsorption on a cellulosic material followed by intein self-cleavage or ethylene glycol elution. The details of recombinant enzyme sources, purification methods, and specific activities are present in Table 1. SDS-page analysis of the purified recombinant enzymes is shown in Fig. 2.

In our previous study (Wang et al., 2011), two enzymes no. 9 enzyme transketolase (TK) and no. 12 enzyme aldolase (ALD) from *T. maritima* had very low specific activities of 0.21 U/mg at 25 °C and 1.32 U/mg at 60 °C, respectively. By using bioinformatics tools based on protein sequence comparison compared to the reported activities of sequence-similar enzymes in Brenda database, we discovered two high-activity enzymes: transketolase (TK) and aldolase (ALD) from *T. thermophilus* HB27, exhibiting approximately 6 times and 23 times those from *T. maritima*, respectively (Table 1). Their opening reading frames were Ttc1896 and Ttc1414, respectively, according to the Kyoto Encyclopedia of Genes and Genomes (KEGG). These data suggested that more high-activity enzyme building blocks could be discovered from rapidly-expanding (mega) genomes.

3.3. Sucrose hydrogen production

To validate the synthetic pathway design, the fifteen enzymes (Table 1) were put into a bioreactor at 37 °C and 1 atm, where the loading of enzyme nos. 1–5 was 5 U/mL and that of the other enzymes was 1 U/mL each. When the initial sucrose concentration was 2 mM, dihydrogen evolved as expected (Fig. 3a). The hydrogen generation rate increased rapidly until hour 7.2. The maximum hydrogen rate was 2.98 mmol of H₂ per liter per hour. Due to fast substrate consumption, the hydrogen generation rate decreased over time. In a 100-h batch reaction, the cumulative hydrogen yield was 96.7%, i.e., 23.2 mol of dihydrogen per mole of sucrose (Fig. 3a). In the end of the batch reaction, the sucrose and glucose levels were below the detection limit of the sucrose and glucose assay kit, suggesting the complete utilization of two hexose units of sucrose. *Note:* It was important to wash commercial sucrose phosphorylase before its use because Sigma sucrose phosphorylase contained a significant amount of sucrose. The above experiments demonstrating catabolic water splitting powered by sucrose were repeated four times. The standard deviations of the final hydrogen yields and maximum hydrogen rates were less than 3% and 10%, respectively, in the repeated experiments. When the sucrose concentration was increased from 2 mM to 10 mM at the same enzyme loading, the maximum hydrogen reaction rate was increased by 2.73 fold to 8.14 mmol/L/h (Fig. 3b). When the sucrose concentration was increased

to 50 mM, the maximum hydrogen generation rate was 9.74 mmol/L/h.

4. Discussion

One of the most important features in in vitro biosystems is great engineering flexibility—enzymatic building blocks from

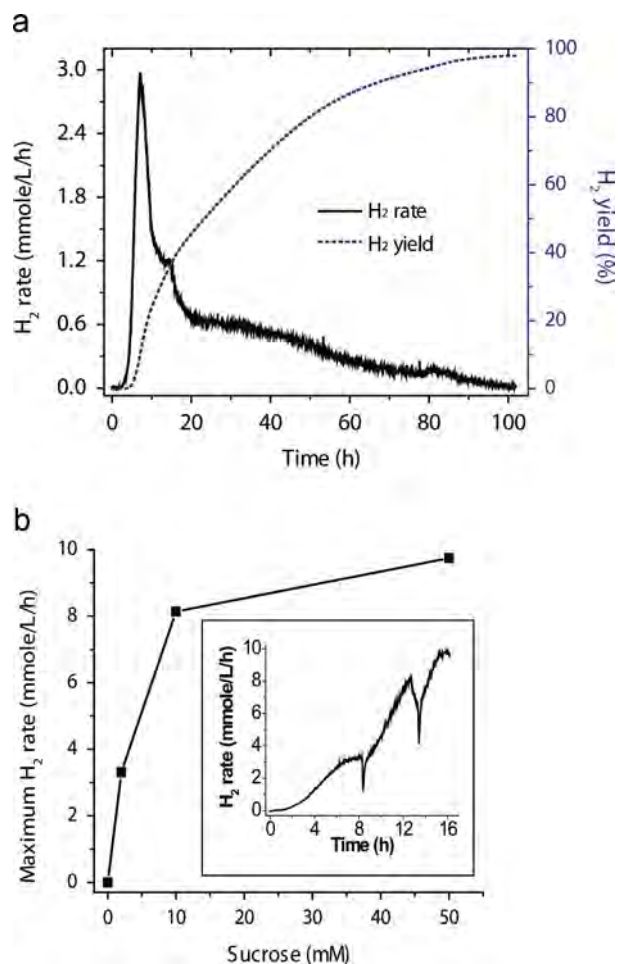


Fig. 3. The profile and yield of dihydrogen generation from 2 mM sucrose, 4 mM Pi and 4 mM (Pi)₆ at 37 °C (a) and the maximum hydrogen generate rate in terms of substrate concentration in a fed-batch experiment (b). The reaction buffer was composed of 100 mM HEPES (pH 7.5), 4 mM NADP⁺, 0.5 mM thiamine pyrophosphate, 10 mM MgCl₂ and 0.5 mM MnCl₂, along with the fifteen enzymes.

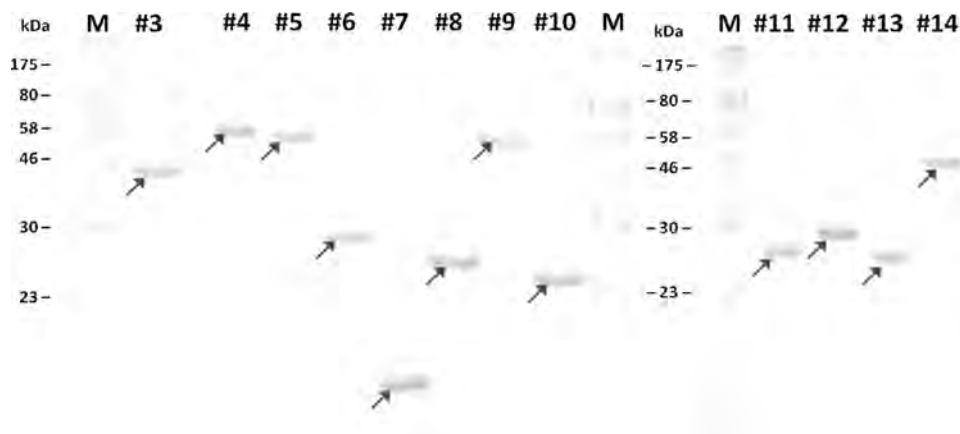


Fig. 2. SDS-PAGE analysis of the 12 purified thermophilic enzymes from nos. 3 to 14.

different sources can be easily assembled together and most of them are highly exchangeable (Guterl et al., 2012; Ye et al., 2012; Zhang et al., 2010). Previous enzymatic hydrogen experiments were accomplished by combining enzymes isolated from rabbit, spinach, archaeobacterium, yeast and *E. coli* into an enzyme cocktail (Woodward et al., 2000; Zhang et al., 2007). Recombinant thermophilic enzymes can be regarded as important standardized building blocks of in vitro synthetic biology projects. In this study, the newly discovered ALD from *T. thermophilus* was 23 times the previously used one from *T. maritima*. As a result, this replacement saved ~29% of proteins in the total protein mass loading. This data suggested that great enzyme cost saving could be accomplished by the discovery or engineering of high-activity enzyme building blocks.

Enzymatic hydrogen generation rates based on hexoses have been accelerated from 0.21 mmol/L/h (Woodward et al., 2000) to 9.74 mmol/L/h by nearly 50 fold. Compared to our previous work – hydrogen production from pentose xylose (Martín del Campo et al., 2013), this experiment showed a 4.4-fold rate enhancement. The volumetric productivity of 9.74 mmol of H₂/L/h equaled the volumetric sugar utilization rate of ca. 0.15 g of hexose consumed/L/h, comparable to some dark hydrogen microbial fermentations (Rittmann and Herwig, 2012) and far higher than those of photo biological hydrogen production. Further reaction enhancement may be conducted by increasing the reaction temperature, the use of small-size NAD-similar biomimetic cofactors for fast mass transfer (Campbell et al., 2012; Rollin et al., 2013), optimizing enzyme loading and ratios (Ardao and Zeng, 2013), the use of substrate-channeling synthetic metabolons (Chen and Silver, 2012; You et al., 2012a), and the discovery of more high-activity enzyme building blocks (e.g., TtcALD and TtcTK in this study).

The potential cost of hydrogen produced from sucrose and water includes expenditure of the consumable substrate (i.e., sucrose), enzymes, coenzyme (i.e., NADP), and buffer, capital investment, product separation as well (Tufvesson et al., 2011). Like the production of most biocommodities (Zhang, 2010), sucrose could account for more than a half of the selling price of hydrogen when all biocatalysts are fully developed (Lynd et al., 1999; Zhang, 2009). To decrease enzyme costs, it is essentially vital to increase total turn-over number of all enzymes to more than 10,000,000 mol of product per mole of enzyme or higher (Zhang et al., 2010). To prolong enzyme stability and recycle biocatalysts from the substrate/product/buffer, enzymes could be immobilized on nano-materials (Burton et al., 2002; Ge et al., 2012; Myung et al., 2013). In addition to enhancing enzyme stability, it is urgently needed to replace costly unstable NADP with more stable and less-costly NAD (Morimoto et al., 2014; Steffler et al., 2013) and less cost and more stable biomimics (Paul et al., 2014; Rollin et al., 2013; Ryan et al., 2008). Cofactor engineering of the two key redox enzymes in this pathway, that is, glucose 6-phosphate dehydrogenase and 6-phosphogluconate dehydrogenase, is under way in our lab. Both engineered redox enzymes can work on a low-cost biomimetic cofactor—1-benzyl-3-carbamoyl-pyridium chloride (in preparation for publication). Without the full development of ultra-stable enzymes and biomimetic cofactors, it would be not economically feasible to produce affordable hydrogen from a variety of sugars. However, a great green hydrogen market, for example, hundreds of billion or even trillions of US dollars annually (Zhang, 2009), could motivate more and more R&D efforts in this important field.

5. Conclusions

High-yield hydrogen generation via catabolic water splitting powered by sugars mediated by enzyme cocktail could be a

promising approach to produce green hydrogen. Further improvements in enzyme stability, replacement of labile coenzymes with stable ones associated with redox enzyme engineering, and enhanced enzymatic hydrogen generation rate would be essentially vital to large-scale green hydrogen production.

Acknowledgments

This work was supported by the Shell GameChanger Program, the CALS Biodesign and Bioprocessing Research Center to PZ at Virginia Tech, as well as two NSF STTR I (IIP-1321528) and DOE STTR I (DE-SC0009659TDD) awards to Cell Free Bioinnovations Inc. SM was partially supported by the ICTAS Scholar Program. JR was supported by the Department of Defense through the National Defense Science and Engineering Graduate (NDSEG) Program. SC and MA were supported by the Division of Chemical Sciences, Geosciences and Biosciences, Office of Basic Energy Sciences of the U.S. Department of Energy (grant DE-FG05-95ER20175).

References

- Agapakis, C., Ducat, D., Boyle, P., Wintermute, E., Way, J., Silver, P., 2010. Insulation of a synthetic hydrogen metabolism circuit in bacteria. *J. Biol. Eng.* 4, 3.
- Ardao, I., Zeng, A.-P., 2013. In silico evaluation of a complex multi-enzymatic system using one-pot and modular approaches: application to the high-yield production of hydrogen from a synthetic metabolic pathway. *Chem. Eng. Sci.* 87, 183–193.
- Armaroli, N., Balzani, V., 2011. The hydrogen issue. *ChemSusChem* 4, 21–36.
- Artero, V., Chavarot-Kerlidou, M., Fontecave, M., 2011. Splitting water with cobalt. *Angew. Chem. Int. Ed.* 50, 7238–7266.
- Barber, J., Tran, P.D., 2013. From natural to artificial photosynthesis. *J. R. Soc. Interface* 10, 81.
- Bujara, M., Schümperli, M., Pellaux, R., Heinemann, M., Panke, S., 2011. Optimization of a blueprint for *in vitro* glycolysis by metabolic real-time analysis. *Nat. Chem. Biol.* 7, 271–277.
- Burton, S.G., Cowan, D.A., Woodley, J.M., 2002. The search for the ideal biocatalyst. *Nat. Biotechnol.* 20, 37–45.
- Campbell, E., Meredith, M., Minteer, S.D., Banta, S., 2012. Enzymatic biofuel cells utilizing a biomimetic cofactor. *Chem. Commun.* 48, 1898–1900.
- Chandrayan, S.K., McTernan, P.M., Hopkins, R.C., Sun, J.S., Jenney, F.E., Adams, M.W.W., 2012. Engineering hyperthermophilic archaeon *Pyrococcus furiosus* to overproduce its cytoplasmic NiFe-hydrogenase. *J. Biol. Chem.* 287, 3257–3264.
- Chen, A.H., Silver, P.A., 2012. Designing biological compartmentalization. *Trends Cell Biol.* 22, 662–670.
- Chou, C.-J., Jenney Jr, F.E., Adams, M.W.W., Kelly, R.M., 2008. Hydrogenesis in hyperthermophilic microorganisms: implications for biofuels. *Metab. Eng.* 10, 394–404.
- Ducat, D.C., Sachdeva, G., Silver, P.A., 2011. Rewiring hydrogenase-dependent redox circuits in cyanobacteria. *Proc. Nat. Acad. Sci. U.S.A.* 108, 3941–3946.
- Esswein, A.J., Nocera, D.G., 2007. Hydrogen production by molecular photocatalysis. *Chem. Rev.* 107, 4022–4047.
- Ge, J., Lei, J., Zare, R.N., 2012. Protein-inorganic hybrid nanoflowers. *Nat. Nano* 7, 428–432.
- Goerke, A.R., Loening, A.M., Gambhir, S.S., Swartz, J.R., 2008. Cell-free metabolic engineering promotes high-level production of bioactive *Gaussia* princeps luciferase. *Metab. Eng.* 10, 187–200.
- Guterl, J.-K., Garbe, D., Carsten, J., Steffler, F., Sommer, B., Reiß, S., Philipp, A., Haack, M., Rühmann, B., Ketting, U., Brück, T., Sieber, V., 2012. Cell-free metabolic engineering—production of chemicals via minimized reaction cascades. *ChemSusChem* 5, 2165–2172.
- Hodgman, C.E., Jewett, M.C., 2012. Cell-free synthetic biology: thinking outside the cell. *Metab. Eng.* 14, 261–269.
- Huang, S.Y., Zhang, Y.-H.P., Zhong, J.J., 2012. A thermostable recombinant transaldolase with high activity over a broad pH range. *Appl. Microbiol. Biotechnol.* 93, 2403–2410.
- Iwuchukwu, I.J., Vaughn, M., Myers, N., O'Neill, H., Frymier, P., Bruce, B.D., 2009. Self-organized photosynthetic nanoparticle for cell-free hydrogen production. *Nat. Nanotech.* 5, 73–79.
- Jung, G.Y., Stephanopoulos, G., 2004. A functional protein chip for pathway optimization and *in vitro* metabolic engineering. *Science* 304, 428–431.
- Korman, T.P., Sahachartsiri, B., Li, D., Vinokur, J.M., Eisenberg, D., Bowie, J.U., 2014. A synthetic biochemistry system for the *in vitro* production of isoprene from glycolysis intermediates. *Protein Sci.* , <http://dx.doi.org/10.1002/pro.2436>.
- Krutsakorn, B., Honda, K., Ye, X., Imagawa, T., Bei, X., Okano, K., Ohtake, H., 2013. *in vitro* production of *n*-butanol from glucose. *Metab. Eng.* 20, 84–91.
- Kuroda, A., Nomura, K., Ohtomo, R., Kato, J., Ikeda, T., Takiguchi, N., Ohtake, H., Kornberg, A., 2001. Role of inorganic polyphosphate in promoting ribosomal protein degradation by the Lon protease in *E. coli*. *Science* 293, 705–708.

- Liao, H.H., Myung, S., Zhang, Y.-H.P., 2012. One-step purification and immobilization of thermophilic polyphosphate glucokinase from *Thermobifida fusca* YX: glucose-6-phosphate generation without ATP. *Appl. Microbiol. Biotechnol.* 93, 1109–1117.
- Lynd, L.R., Wyman, C.E., Gerngross, T.U., 1999. Biocommodity engineering. *Biotechnol. Prog.* 15, 777–793.
- Maeda, T., Sanchez-Torres, V., Wood, T.K., 2012. Hydrogen production by recombinant *Escherichia coli* strains. *Microb. Biotechnol.* 5, 214–225.
- Martín del Campo, J.S., Rollin, J., Myung, S., Chun, Y., Chandrayan, S., Patiño, R., Adams, M.W.W., Zhang, Y.-H.P., 2013. High-yield production of dihydrogen from xylose by using a synthetic enzyme cascade in a cell-free system. *Angew. Chem. Int. Ed.* 52, 4587–4590.
- Morimoto, Y., Honda, K., Ye, X., Okano, K., Ohtake, H., 2014. Directed evolution of the thermostable malic enzyme for improved malate production. *J. Biosci. Bioeng.* 117, 147–152.
- Mubeen, S., Lee, J., Singh, N., Kramer, S., Stucky, G.D., Moskovits, M., 2013. An autonomous photosynthetic device in which all charge carriers derive from surface plasmons. *Nat. Nanotechnol.* 8.
- Myung, S., Wang, Y.R., Zhang, Y.-H.P., 2010. Fructose-1,6-bisphosphatase from a hyper-thermophilic bacterium *Thermotoga maritima*: characterization, metabolic stability and its implications. *Proc. Biochem.* 45, 1882–1887.
- Myung, S., You, C., Zhang, Y.-H.P., 2013. Recyclable cellulose-containing magnetic nanoparticles: immobilization of cellulose-binding module-tagged proteins and synthetic metabolon featuring substrate channeling. *J. Mater. Chem. B* 1, 4419–4427.
- Myung, S., Zhang, X.-Z., Zhang, Y.-H.P., 2011. Ultra-stable phosphoglucose isomerase through immobilization of cellulose-binding module-tagged thermophilic enzyme on low-cost high-capacity cellulosic adsorbent. *Biotechnol. Prog.* 27, 969–975.
- Myung, S., Zhang, Y.-H.P., 2013. Non-complexed four cascade enzyme mixture: simple purification and synergistic co-stabilization. *PLoS One* 8, e61500.
- Navarro, R.M., Pena, M.A., Fierro, J.L.G., 2007. Hydrogen production reactions from carbon feedstocks: fossil fuels and biomass. *Chem. Rev.* 107, 3952–3991.
- Nelson, D.L., Cox, M.M., 2008. *Lehninger Principles of Biochemistry*, fifth ed. WH Freeman, New York.
- Panke, S., Held, M., Wubbolts, M., 2004. Trends and innovations in industrial biocatalysis for the production of fine chemicals. *Curr. Opin. Biotechnol.* 15, 272–279.
- Paul, C.E., Arends, I.W.C.E., Hollmann, F., 2014. Is simpler better? Synthetic nicotinamide cofactor analogues for redox chemistry. *ACS Catal.* 4, 788–797.
- Qi, P., You, C., Zhang, Y.H.P., 2014. One-pot enzymatic conversion of sucrose to synthetic amylose by using enzyme cascades. *ACS Catal.* 4, 1311–1317.
- Rittmann, S., Herwig, C., 2012. A comprehensive and quantitative review of dark fermentative biohydrogen production. *Microb. Cell Fact.* 11, 115.
- Rollin, J.A., Tam, W., Zhang, Y.-H.P., 2013. New biotechnology paradigm: cell-free biosystems for biomanufacturing. *Green Chem.* 15, 1708–1719.
- Ryan, J.D., Fish, R.H., Clark, D.S., 2008. Engineering cytochrome P450 enzymes for improved activity towards biomimetic 1,4-NADH cofactors. *ChemBioChem* 9, 2579–2582.
- Steffler, F., Guterl, J.-K., Sieber, V., 2013. Improvement of thermostable aldehyde dehydrogenase by directed evolution for application in synthetic cascade biomanufacturing. *Enzyme Microb. Technol.* 53, 307–314.
- Sun, F.F., Zhang, X.Z., Myung, S., Zhang, Y.-H.P., 2012. Thermophilic *Thermotoga maritima* ribose-5-phosphate isomerase RpiB: optimized heat treatment purification and basic characterization. *Protein Expression Purif.* 82, 302–307.
- Swartz, J.R., 2013. Cell-free bioprocessing. *Chem. Eng. Prog.* 2013, 40–45.
- Tufvesson, P.R., Lima-Ramos, J., Nordblad, M., Woodley, J.M., 2011. Guidelines and cost analysis for catalyst production in biocatalytic processes. *Org. Process Res. Dev.* 15, 266–274.
- Wang, R.-Y., Shi, Z.-Y., Chen, J.-C., Wu, Q., Chen, G.-Q., 2012. Enhanced co-production of hydrogen and poly-(R)-3-hydroxybutyrate by recombinant PHB producing *E. coli* over-expressing hydrogenase 3 and acetyl-CoA synthetase. *Metab. Eng.* 14, 496–503.
- Wang, Y., Huang, W., Sathitsuksanoh, N., Zhu, Z., Zhang, Y.-H.P., 2011. Biohydrogenation from biomass sugar mediated by *in vitro* synthetic enzymatic pathways. *Chem. Biol.* 18, 372–380.
- Wang, Y., Zhang, Y.-H.P., 2010. A highly active phosphoglucomutase from *Clostridium thermocellum*: cloning, purification, characterization, and enhanced thermostability. *J. Appl. Microbiol.* 108, 39–46.
- Wells, M.A., Mercer, J., Mott, R.A., Pereira-Medrano, A.G., Burja, A.M., Radianingtyas, H., Wright, P.C., 2011. Engineering a non-native hydrogen production pathway into *Escherichia coli* via a cyanobacterial [NiFe] hydrogenase. *Metab. Eng.* 13, 445–453.
- Woodward, J., Orr, M., Cordray, K., Greenbaum, E., 2000. Enzymatic production of biohydrogen. *Nature* 405, 1014–1015.
- Xu, Y., Masuko, S., Takiyeddin, M., Xu, H., Liu, R., Jing, J., Mousa, S.A., Linhardt, R.J., Liu, J., 2011. Chemoenzymatic synthesis of homogeneous ultralow molecular weight heparins. *Science* 334, 498–501.
- Ye, X., Honda, K., Sakai, T., Okano, K., Omasa, T., Hirota, R., Kuroda, A., Ohtake, H., 2012. Synthetic metabolic engineering—a novel, simple technology for designing a chimeric metabolic pathway. *Microb. Cell Fact.* 11, 120.
- Ye, X., Wang, Y., Hopkins, R.C., Adams, M.W.W., Evans, B.R., Mielenz, J.R., Zhang, Y.-H.P., 2009. Spontaneous high-yield production of hydrogen from cellulosic materials and water catalyzed by enzyme cocktails. *ChemSusChem* 2, 149–152.
- You, C., Chen, H., Myung, S., Sathitsuksanoh, N., Ma, H., Zhang, X.-Z., Li, J., Zhang, Y.-H.P., 2013. Enzymatic transformation of nonfood biomass to starch. *Proc. Nat. Acad. Sci. U.S.A.* 110, 7182–7187.
- You, C., Myung, S., Zhang, Y.-H.P., 2012a. Facilitated substrate channeling in a self-assembled trifunctional enzyme complex. *Angew. Chem. Int. Ed.* 51, 8787–8790.
- You, C., Zhang, X.-Z., Zhang, Y.-H.P., 2012b. Simple cloning via direct transformation of PCR product (DNA multimer) to *Escherichia coli* and *Bacillus subtilis*. *Appl. Environ. Microbiol.* 78, 1593–1595.
- You, C., Zhang, Y.H.P., 2014. Annexation of a high-activity enzyme in a synthetic three-enzyme complex greatly decreases the degree of substrate channeling. *ACS Synth. Biol.* 10.1021/sb4000993.
- Zhang, Y.-H.P., 2009. A sweet out-of-the-box solution to the hydrogen economy: is the sugar-powered car science fiction? *Energy Environ. Sci.* 2, 272–282.
- Zhang, Y.-H.P., 2010. Production of biocommodities and bioelectricity by cell-free synthetic enzymatic pathway biotransformations: challenges and opportunities. *Biotechnol. Bioeng.* 105, 663–677.
- Zhang, Y.-H.P., Evans, B.R., Mielenz, J.R., Hopkins, R.C., Adams, M.W.W., 2007. High-yield hydrogen production from starch and water by a synthetic enzymatic pathway. *PLoS One* 2, e456.
- Zhang, Y.-H.P., Sun, J.-B., Zhong, J.-J., 2010. Biofuel production by *in vitro* synthetic pathway transformation. *Curr. Opin. Biotechnol.* 21, 663–669.
- Zhu, Z.G., Kin Tam, T., Sun, F., You, C., Zhang, Y.-H.P., 2014. A high-energy-density sugar biobattery based on a synthetic enzymatic pathway. *Nat. Commun.* 5, 3026.
- Zhu, Z.G., Sun, F., Zhang, X., Zhang, Y.-H.P., 2012. Deep oxidation of glucose in enzymatic fuel cells through a synthetic enzymatic pathway containing a cascade of two thermostable dehydrogenases. *Biosens. Bioelectron.* 36, 110–115.